Rockefeller University
Report No. DOE/ER/40033-36

(RU 81/A-34)

DIFFRACTION DISSOCIATION and THE DIRECT HADRONIC INTERACTION OF THE PHOTON

K. Goulianos*

The Rockefeller University
New York, N.Y. 10021, U.S.A.

ABSTRACT:

We report a measurement of the inclusive diffraction dissociation cross section of $\sim$ 100 GeV photons on hydrogen; we test the finite mass sum rule and, comparing with pion dissociation data, we test factorization. Our results are interpreted as providing a measurement of the direct, non "vector meson dominance" hadronic interaction of the photon.

* Report on Fermilab Experiment E-612:

T.J. Chapin, R.L. Cool, K. Goulianos, K.A. Jenkins,
J.P. Silverman+, G.R. Snow, H. Sticker and S.N. White
The Rockefeller University

and

Yue Hua Chou
Institute of High Energy Physics, Beijing
The People's Republic of China

Presented at
The XVIIIth Rencontre de Moriond
La Plagne (Savoie, France)
January 23-29, 1983

+ Present Address: Thomas J. Watson Research Center
Yorktown Heights, NY 10598

In an experiment performed at Fermilab, E-612, we measured the inclusive diffraction dissociation cross section $d^2\sigma/dtdM_X^2$ of $\sim$100 GeV photons incident on protons,

$$\gamma + p \rightarrow X + p \tag{1}$$

in the kinematic range $0.02 < |t| < 0.1$ $(GeV/c)^2$ and $M_X^2/s \lesssim 0.1$. As a control experiment, we also measured, in the same apparatus, the pion diffraction dissociation cross section,

$$\pi^- + p \rightarrow X + p \tag{2}$$

at 100 GeV/c. Pion dissociation has been measured previously[1]; this experiment represents the first measurement of inclusive photon dissociation at high energies.

We find that, for $M_X^2 > 4$ GeV^2, the differential cross sections for both reactions vary as $1/M_X^2$ and are exponential in t, a behavior consistent with that predicted by a simple triple-Pomeron Regge type amplitude. By applying the finite mass rum rule to the photon data, and by comparing the photon with the pion data to test factorization, we conclude that the photon has a direct hadronic interaction in addition to that described by the well-known[2] vector-meson dominance model (VDM).

The experiment was performed in the tagged photon beam of Fermilab. The photons were obtained from an 148 GeV/c electron beam incident on a 20% tungsten radiator. The energy of the photons was determined to $\pm$ 2% by bending the radiating electrons out of the beam and measuring their energy with lead glass counters. Typically, the photon beam contained $\sim 1 \times 10^6$ tagged photons per pulse in the energy range $75 < E_\gamma < 148$ GeV. With the Bremsstrahlung energy spectrum varying as 1/E, the mean energy of the photons was $\sim$100 GeV. The photon flux was limited by the rate capability of our detector. Double photon production in the radiator was monitored by a total absorption counter which, placed in the photon beam downstream of our apparatus, measured the total energy of the non-interacting photons. The pion beam was formed by intercepting the secondary neutral beam, which created the electrons, with a 5 cm lead brick. An electromagnetic halo accompanying the beam limited the acceptable flux of pions to $\sim 5 \times 10^4$ per pulse. The pulse repetition period of the machine was $\sim$10 sec and the beam spill time $\sim$ 1 sec. Data were collected in two runs of approximately equal duration, one during the month of January and the other during March of 1982.

The experimental technique consisted in measuring the kinetic energy and polar angle of recoil protons in the region $10 < T < 50$ MeV and $45^0 < \theta < 90^0$. The variables t and M_x^2 were then determined from T, θ and p_o, the momentum of the beam particle, using the equations

$$t = -2M_pT \tag{3}$$

$$M_x^2 = M_o^2 + 2p_o \sqrt{|t|} \left(\cos\theta - \sqrt{|t|}/2M_p\right) \tag{4}$$

where M_p is the mass of the recoil proton and M_o the mass of the incident particle.

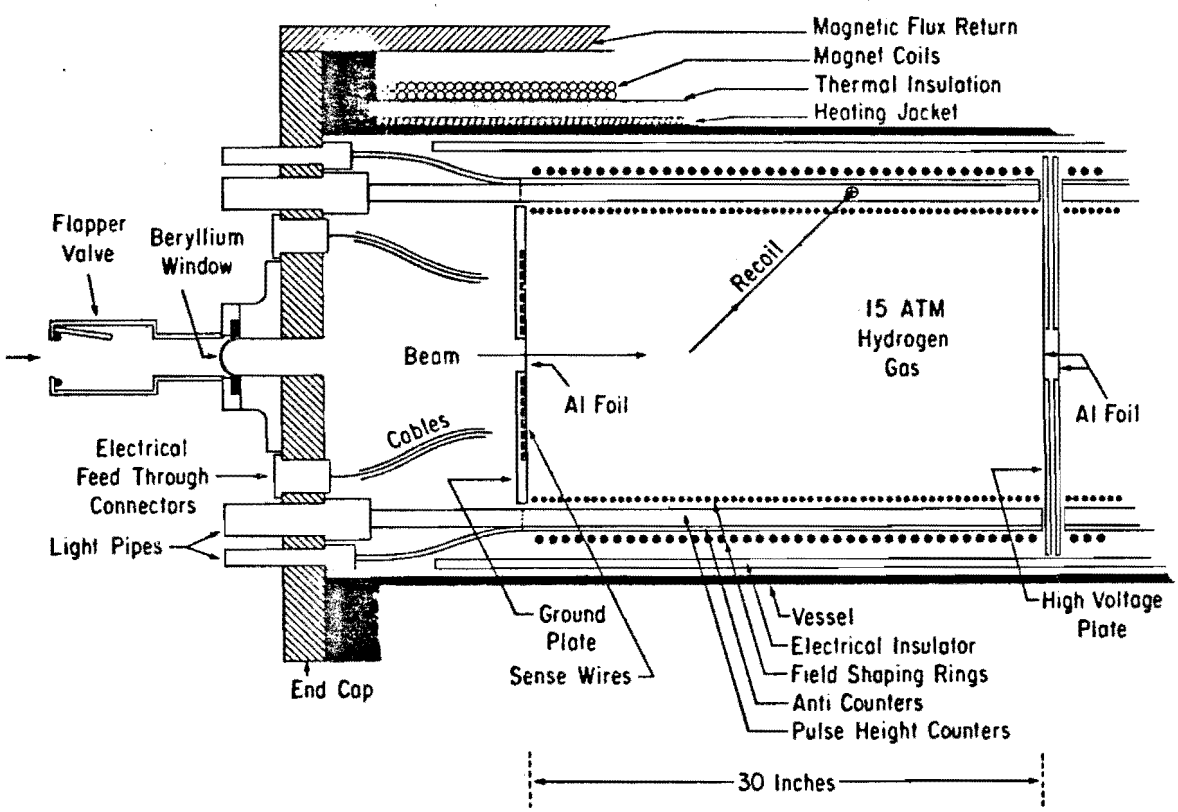

FIG. 1 - TREAD (The Recoil Energy and Angle Detector).

The apparatus, TREAD (The Recoil Energy and Angle Detector), shown in Figure 1, was described in detail in a previous publication[3]. It is a hydrogen filled, high pressure time projection chamber (TPC) that served both as target and as detector of the recoil protons. It consists of two cylindrical drift regions in tandem, each 45 cm in diameter and 75 cm long. The beam entered the TPC along the axis of the cylinder through a 0.75 mm thick, 5 cm dia. beryllium window and exited through a 2 mm thick, 20 cm dia. aluminum window. The dissociation products also exited through the aluminum

window, whereupon their charged multiplicity was determined by measuring the pulse height in two scintillation counters. This technique was used previously[4] by some members of this group in a hadron experiment, E-396, performed at Fermilab's meson laboratory. The energy of the recoil protons was determined by stopping them in 2.5 cm thick plastic scintillation counters located inside the pressure vessel. The energy loss in the hydrogen gas, dE/dx, was obtained from the pulse height of the sense wires. Recoiling protons were identified by comparing T with dE/dx.

In this report we present the result of the analysis of the data collected during March 1982. The data obtained in January of 1982 are currently being analyzed. Details of the analysis will be given elsewhere[5]. Basically, after track selection and appropriate cuts in dE/dx versus E and in recoil time of flight, the background was negligible.

Figure 2 is a scatter plot of the recoil kinetic energy against dE/dx for the photon data. The prominent band represents the recoil protons for which the energy loss varies as 1/T. Multiplying dE/dx by T yields a constant which is proportional to the mass of the recoil particle. Figure 3 is a histogram of (dE/dx) • T . The peak consists of recoil protons. Its width is mainly due to the dE/dx measurement resolution.

The M_x^2 distributions of the pion and photon data, normalized respectively to the $\pi^- p$ and γp total cross sections, are shown in Figure 4. The data, representing about 7,500 pion and 8,500 photon events, are plotted against the cross-symmetric variable ν ,

$$\nu = M_x^2 - M_o^2 - t \tag{5}$$

where M_o is the mass of the incident particle. The width of the pion elastic peak at $\nu \cong 0$ and of the ρ-meson peak at $\nu \cong 0.6\ \mathrm{GeV}^2$ are mostly due to the measurement resolution. The resolution is poorer in the photon data, which were collected over a period of one month, than in the pion data, collected during one day. In the Regge model, under the assumption of factorization, the high mass diffraction dissociation cross-section arising from a triple-Pomeron term can be written as

$$\frac{d^2\sigma^{hp}}{dt d\nu} = \frac{\beta_{hP}(o)\ \ \beta^2_{pP}(t)\ \ G_{PPP}(t)}{16\pi\nu} \tag{6}$$

where h represents the hadron dissociating on the proton and P represents

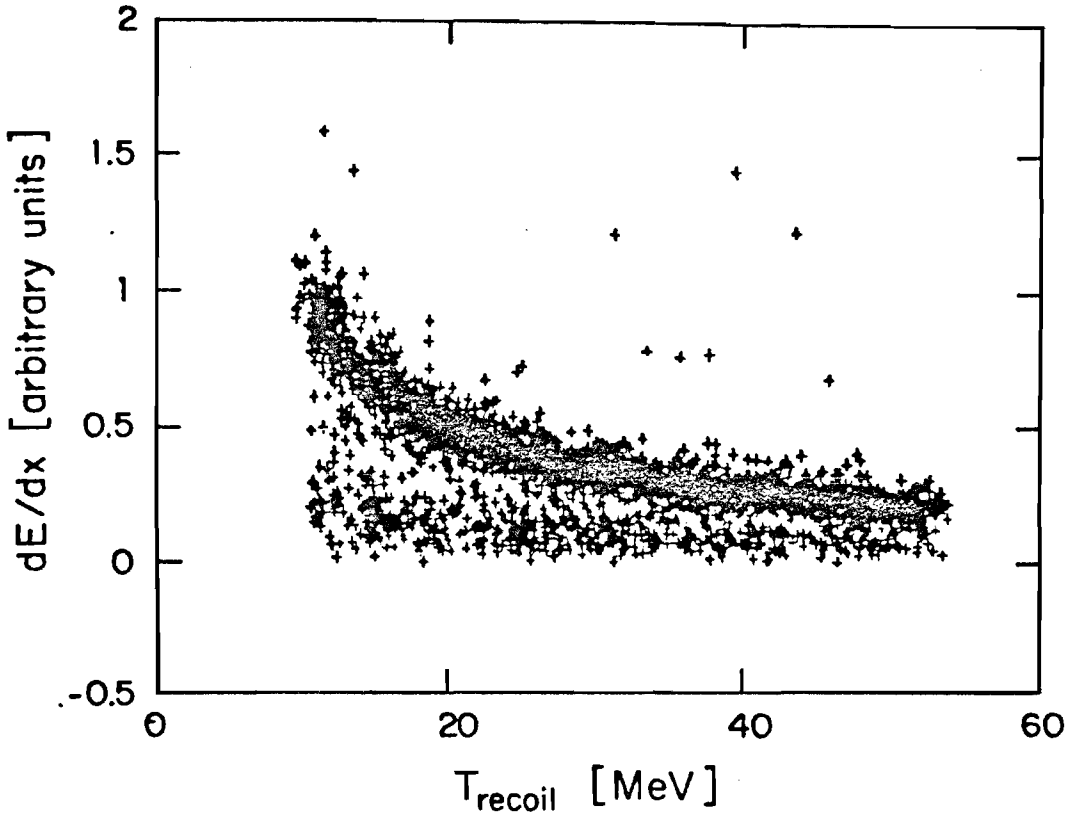

FIG. 2 - Recoil particle energy loss, dE/dx, versus kinetic energy. The prominent band represents recoil protons.

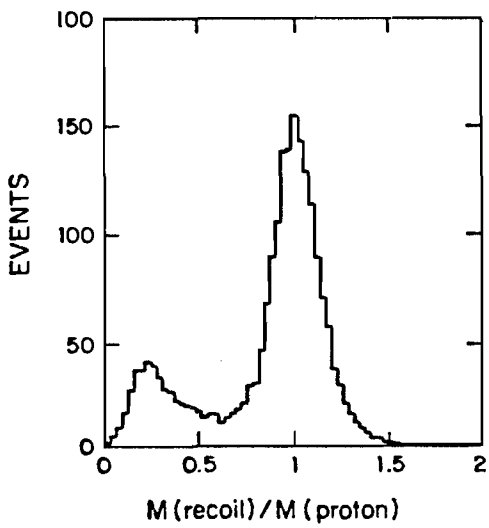

FIG. 3 - Recoil particle energy loss times kinetic energy, (dE/dx)·T. This product is proportional to the mass of the recoil particle. The position of the peak is normalized to unity so that the abseissa represents M(recoil)/M(proton).

the Pomeron. In the same model, the total cross section at high energies is given by

$$\sigma_T^{hp} = \beta_{hP}(o) \; \beta_{pP}(o) \qquad (7)$$

In writing (6) and (7), we have taken, for simplicity, the Pomeron trajectory to be $\alpha(o) = 1$ and, because of our small t values, the slope of the trajectory to be $\alpha'(t) = 0$. The ratio of the diffractive to the total cross section,

$$\frac{d^2\sigma^{hp}/dt\, d\nu}{\sigma_T^{hp}} = \frac{\beta_{pp}^2(t)}{\beta_{pp}(o)} \frac{G_{ppp}(t)}{16\pi\nu} \tag{8}$$

is independent of the incident particle type. The $1/\nu$ behavior predicted by Eq. (6) and the scaling of the diffractive to the total cross section given by Eq. (8) have been found to hold for $\pi^{\pm}$, $K^{\pm}$, and $p^{\pm}$ hadrons dissociating on protons[1]. Figure 4 shows that the high mass diffractive photon cross section is $\sim$15% higher than the pion cross section (scaled by the corresponding σ_T). This could, of course, be considered as a positive test of factorization in view of the fact that the photon total cross section is $\sim$200 times smaller than the pion cross section. However, this discrepancy finds a logical explanation in the framework of the vector-meson dominance model.

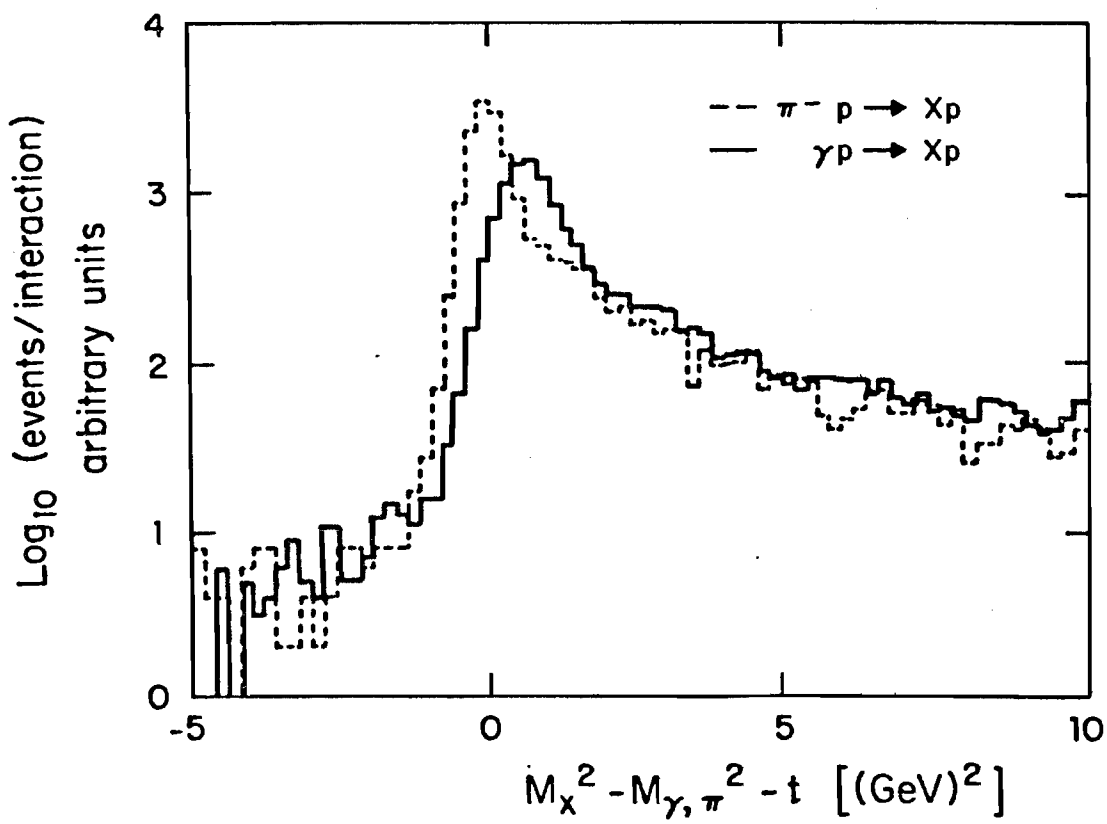

FIG. 4 - M_X^2 distributions for $\gamma(\pi^-) + p \to X + p$ at 100 GeV/c and $0.02 < |t| < 0.1$ $(GeV/c)^2$, normalized to the corresponding total cross sections, $\gamma(\pi^-) + p \to$ anything.

In its original version, the VDM states that the hadronic interaction of the photon is transmitted through the coupling of the photon to the vector mesons ρ, ω and ϕ. For simplicity, we will consider only the ρ-meson in this discussion. A photon cannot transform into a ρ in free space. Conversion to ρ requires an energy change $\Delta E = M_\rho^2/2E_\gamma$. For 100 GeV photons, ΔE = 3 MeV. Through the uncertainty principle, $\Delta E \cdot \Delta t \sim 1$, this energy shift corresponds to a time interval which is large compared to the characteristic time of strong interactions set by the mass of the pion (140 MeV). Thus, high energy photons can live in and interact with nuclear matter as "free" ρ-mesons. Of course, photons can also interact directly. Therefore, the effective "incident photon" mass, M_0^2, lies somewhere between zero and M_ρ^2. Assuming that there is no interference between the γ and ρ amplitudes, the value of M_0^2 is given by

$$M_0^2 = \frac{P_\gamma \sigma_\gamma^D M_\gamma^2 + P_\rho \sigma_\rho M_\rho^2}{P_\gamma \sigma_\gamma^D + P_\rho \sigma_\rho} = \frac{P_\rho \sigma_\rho M_\rho^2}{\sigma_\gamma^T} \tag{9}$$

where $P_{\gamma,\rho}$ are the probabilities of finding the photon in the $\gamma(M_\gamma^2=0)$ or $\rho(M_\rho^2 = 0.59\ \mathrm{GeV}^2)$ states and σ_γ^D is the "direct" γ total cross section. The VDM assumes that $P_\rho \sigma_\rho \gg P_\gamma \sigma_\gamma$ and hence $M_0^2 \cong M_\rho^2$. Had we used M_ρ^2 instead of M_γ^2 in Figure 4, the photon data would be in agreement with the pion data. Thus, assuming the validity of factorization and of the Regge model, this result supports the VDM. However, it is not sensitive enough to rule out a direct photon interaction of $\sim$20% which is required to explain the shadowing of photons in nuclei[2]. Such an interaction is also desirable in the simple VDM which can account for only $\sim$80% of the photon total cross section, although this inadequacy can be corrected by introducing the generalized VDM[2]. A more sensitive measurement of M_0^2, and hence of the direct photon interaction, is provided by our data through the application of the finite mass sum rule (FMSR).

The FMSR[6] relates the high mass diffractive cross section to the low mass "resonance region." It states that the fit to the large ν differential cross section, $d^2\sigma/dtd\nu$, multiplied by ν represents the average behavior of $\nu(d^2\sigma/dtd\nu)$ in the low mass region, including elastic scattering for which $\nu = |t|$:

$$|t| \frac{d\sigma_{e\ell}}{dt} + \int_0^{\nu'} \nu \frac{d^2\sigma}{dtd\nu} d\nu = \int_0^{\nu'} \nu \left(\frac{d^2\sigma}{dtd\nu}\right)_{\text{fit at large } \nu} d\nu \tag{10}$$

The value of ν' must lie beyond the "resonance region" but is otherwise arbitrary. However, the lower the value of ν' the more sensitive the test of the FMSR. The elastic contribution appears explicitly in Eq. (10). Experimentally, due to resolution in the measurement of M_x^2, elastic scattering appears as a peak of finite width in ν centered around $\nu = |t|$. In applying the FMSR, the elastic events can be treated just as the inelastic ones; namely, by multiplying the apparent cross section $d^2\sigma/dtd\nu$ by $\nu = M_x^2 - M_o^2 + |t|$ and integrating over ν down to values which are low enough to include all events. For a resolution broadened peak which is symmetric around $M_x = M_o$, the elastic events in this procedure are, in effect, multiplied by $|t|$, as required by the FMSR. Thus, in applying the FMSR to experimental data, Eq. (10) can be written as

$$R \equiv \frac{\int^{\nu'} \nu \frac{d^2\sigma}{dtd\nu} d\nu}{\int_o^{\nu'} \nu \left(\frac{d^2\sigma}{dtd\nu}\right)_{\text{fit at large } \nu} d\nu} = 1 \tag{11}$$

where the lower limit of integration in the numberator has been omitted but it is understood that one must sum over all events below ν', including the elastic events that are forced by the resolution to appear at negative values of ν.

Figures 5a and 5b show $\nu(d^2\sigma/dtd\nu)$ for our pion and photon data plotted against $\nu = M_x^2 - M_{\pi,\gamma}^2 + |t|$. For $\nu \gtrsim 4$ GeV^2, our data for both reactions are flat, implying an $1/\nu$ behavior of $d^2\sigma/dtd\nu$ and hence triple-Pomeron dominance in the diffractive cross sections. The $A_1(M^2=1.63)$ and $\rho'(M^2=2.56)$ peaks are clearly visible in the pion and photon data, respectively. Applying the FMSR with $\nu' = 4$ GeV^2, we find $R_\pi = 1.10 \pm 0.05$ and $R_\gamma = 1.43 \pm 0.04$. Clearly, in this straightforward application, the FMSR fails for the photon data. We attribute this failure to the fact that, as discussed previously, the photon interacts partly as a ρ-meson and therefore $\nu = M_x^2 - M_o^2 - t$, where M_o^2 is given by Eq. (9). Treating M_o^2 as a free parameter and demanding the validity of the FMSR, i.e., $R \simeq 1$ in Eq. (10), we find $M_o^2 = 0.46 \pm 0.02$ GeV^2. From Eq. (9), we then find $P_\rho\sigma_\rho/\sigma_\gamma^T = M_o^2/M_\rho^2 = (0.46 \pm 0.02)/0.59 = 0.78 \pm 0.035$ and consequently

$$\sigma_\gamma^D = (0.22 \pm 0.035)\ \sigma_\gamma^T \tag{12}$$

i.e., the direct hadronic photon cross section is 22 ± 3.5% of the total.

As mentioned earlier, this value is in agreement with results on shadowing of photon total cross sections in nuclei and with the fact that the simple VDM accounts for only ∿80% of the total photon cross section.

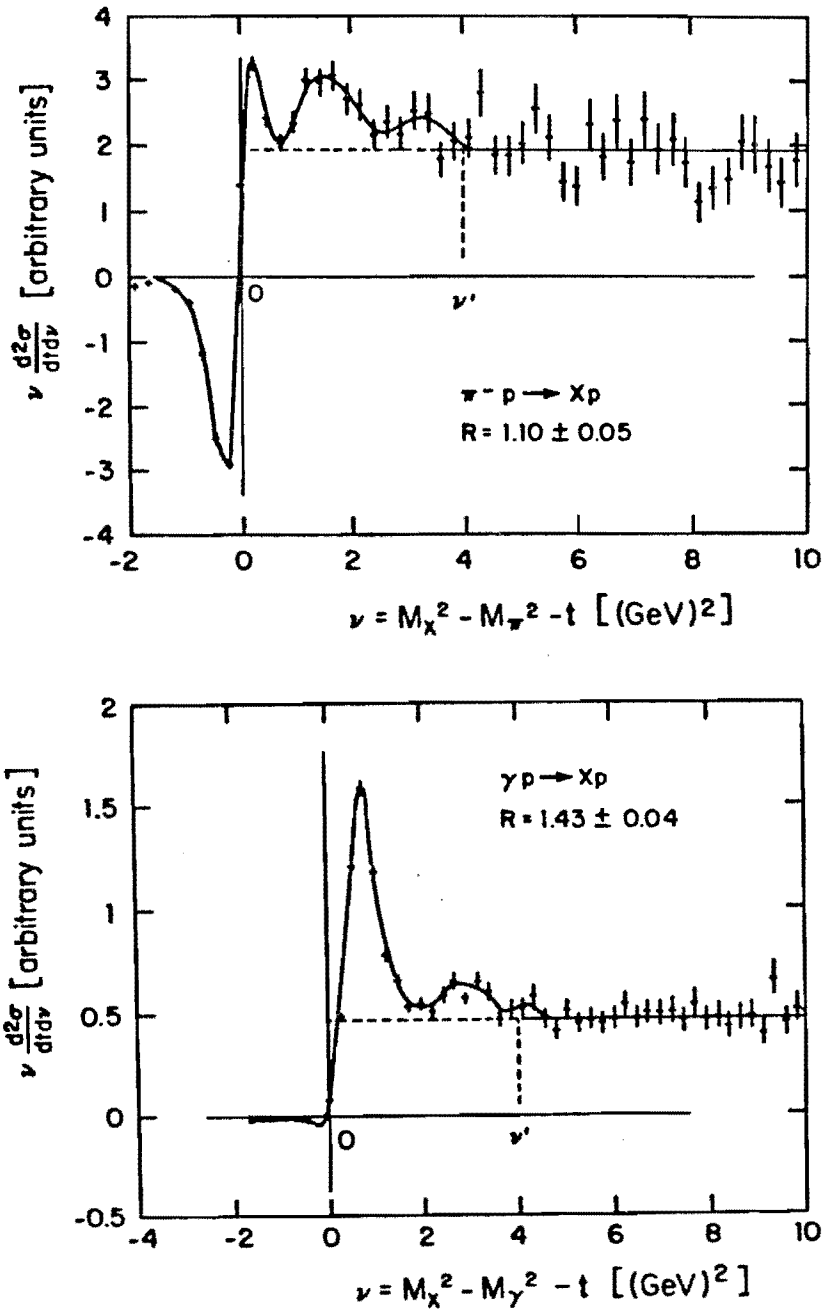

FIG. 5 - Test of the finite mass sum rule: The product $\nu(d^2\sigma/dtd\nu)$, where $\nu = M_X^2 - M_{\pi,\gamma}^2 + |t|$, plotted against ν; (a) for $\pi^- p \rightarrow Xp$ and (b) for $\gamma p \rightarrow Xp$ at 100 GeV/c and $0.02 < |t| < 0.1$ (GeV/c)^2.

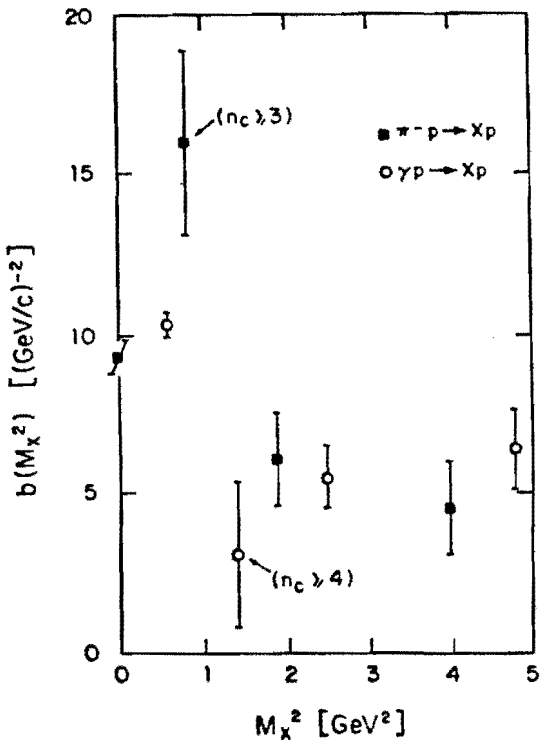

FIG. 6

The slope parameter b as a function of M_X^2 for $\gamma(\pi^-) + p \to X + p$ at 100 GeV/c and $0.02 < |t| < 0.1$ $(GeV/c)^2$.

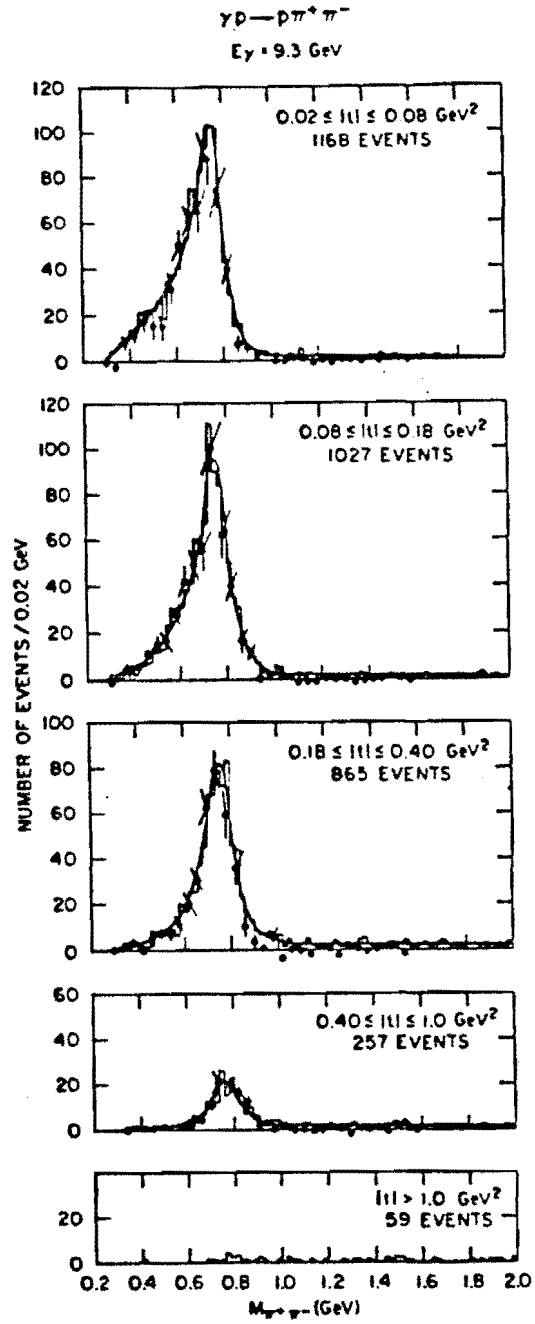

FIG. 7

The "shape of the ρ" as a function of t. (from Reference 2)

The t distributions were fitted to the simple exponential form e^{bt}. Figure 6 shows the slope parameter b as a function of M_X^2. The pion elastic scattering and high mass diffraction slopes are in good agreement with the values of 8.92 ± 0.31 and 4.3 ± 0.7 $(GeV/c)^{-2}$ measured[7] in experiment E-396. The slope at $M_X^2 \cong 0.8$ GeV^2 was obtained from pion data with charged multiplicity ≥ 3 in order to exclude events from the nearby elastic peak. The large value of the slope in this low mass inelastic region is essential in satisfying the FMSR at small values of t. From Eq. (10), it is seen that as $|t| \to 0$ the elastic contribution vanishes; however, due to the large value of the slope of the low mass inelastic region, the relative

contribution of this region increases at small t and the FMSR is satisfied. Our present data are not accurate enough to provide a stringent test of the FMSR as a function of t. Such a test was performed[8] for $pp \to Xp$; it was found that the slope parameter of the low mass region was indeed high and its magnitude was exactly what was required to satisfy the FMSR.

In examining the slope parameters of the photon dissociation data, we observe the following:

(i) The slopes of the high mass photon and pion data are in agreement.

(ii) The slope at the mass of the ρ-meson (M_X^2=0.59) is about one unit higher than the pion elastic scattering slope, although the statistical significance of this difference is not very high.

(iii) There is no increase of the slope in the region $M_X^2 > M_\rho^2$.

The M_X^2 dependence of b does not follow exactly the pattern set by the hadron data. The slope is not higher in the region just above the ρ mass and, in this sense, the ρ' does not correspond to the A_1 enhancement. Following the argument presented previously, it would then appear that the FMSR would be violated at small values of t. However, data from experiments at lower energies (see Fig. 7) indicate that the slope in the mass region $M_X^2 < M_\rho^2$ is higher than the slope of the ρ. Our experimental resolution does not permit us to observe directly this increase of slope at low masses, but indirect evidence is provided by the fact that the measured slope of the ρ is larger than that of pion elastic scattering. Thus, the low mass "tail" of the ρ in $\gamma p \to Xp$ may indeed play the role of the A_1 and N^* (1400) enhancements observed in $\pi p \to Xp$ and $pp \to Xp$, respectively.

As mentioned earlier, we also measured in this experiment the pulse height in two scintillation counters placed downstream of TREAD in order to determine the charged multiplicity of the dissociation products. Figure 8 shows the pulse height spectra f the photon and pion data in the region $3 < M_X^2 < 10$ GeV^2 in units corresponding to minimum ionizing particles. In order to extract the multiplicity distribution, these spectra must be fitted with appropriate Landau functions. However, a direct comparison of the photon and pion data, which in Figure 8 are normalized to the same number of events, already shows that the charged multiplicity distribution has the same mean value and the same width for both reactions. This result is in agreement with the "Universality of Charged Multiplicity Distributions" shown to hold for hadronic masses[9].

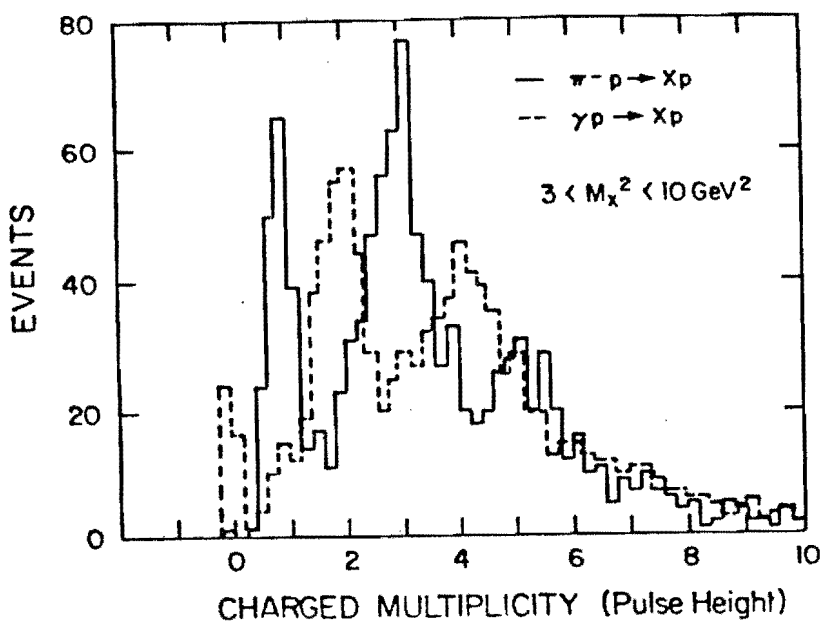

FIG. 8 - Pulse height spectra ("charged multiplicities") of the dissociation products for $\gamma(\pi^-) + p \to X + p$ at 100 GeV/c in the region $3 < M_X^2 < 10$ GeV^2.

In summary, we find that $d^2\sigma/dtd\nu$ for $\gamma(\pi^-) + p \to X + p$ at 100 GeV/c varies as $(1/\nu)\, e^{bt}$, in agreement with a triple-Pomeron amplitude; by testing factorization and the FMSR, we conclude that the effective mass of the incident photon is $M_0^2 = 0.46 \pm 0.02$ GeV^2 and, by comparing with M_ρ^2, we determine the direct, non-VDM hadronic cross section of the photon to be 22 ± 3.5% of the total cross section; from a study of the t-distributions, combined with results from experiments at lower energies, we argue that the low mass "tail" of the ρ-meson is the counterpart of the low mass enhancements A_1 and N^* (1400) observed in $\pi^-(p) + p \to X + p$; finally, from the pulse height spectra in the "multiplicity counters", we verify the universality character of the charged multiplicity distributions for the case of photons.

REFERENCES

1. R.L. Cool, K. Goulianos, S.L. Segler, H. Sticker and S.N. White, Phys. Rev. Letters 47, 701 (1981).

2. T.H. Bauer, D. Spital, D.R. Yennine and F.M. Pipkin, Reviews of Modern Physics 50, 26 (1978).

3. T. Chapin et al., Nuclear Instruments and Methods 197, 305 (1982).

4. R.L. Cool, K. Goulianos, S.L. Segler, H. Sticker and S.N. White, Phys. Rev. Letters 48, 1451 (1982).

5. Gregory Snow, Ph.D. Thesis, Rockefeller University (in preparation).

6. A.I. Sanda, Phys. Rev. D6, 280 (1972); M.B. Einhorn, J. Ellis and J. Finkelstein, ibid. 5, 2063 (1972).

7. R.L. Cool, K. Goulianos, S.L. Segler, G. Snow, H. Sticker and S.N. White, Phys. Rev. D24, 2821 (1981).

8. Y. Akimov et al., Phys. Rev. D14, 3148 (1976).

9. K. Goulianos, H. Sticker and S.N. White, Phys. Rev. Letters 48, 1454 (1982).

ADDENDUM TO PROPOSAL P-670

T.J. Chapin, R.L. Cool, K. Goulianos*, K. Jenkins,
G.R. Snow, H. Sticker and S.N. White

The Rockefeller University
New York, NY 10021

SUMMARY

We propose to extend the study of inclusive pion and photon diffraction dissociation to 300 GeV, and study small t pion elastic scattering from 50 to 300 GeV, using our E-612 apparatus in its present set-up in the Tagged Photon Laboratory during the second part of the 1983-1984 running period.

*Spokesman (Telephone: 212/570-8827)

Proposal P-670 discusses the continuation of experiment E-612 at the Tevatron. At the time P-670 was submitted, we only indicated the general direction in which we would continue the experiment and stated that we would be more specific when results from E-612 became available. About one-half of our E-612 data have now been analyzed and our results are presented in a paper[1] entitled "Diffraction Dissociation and the Direct Hadronic Interaction of the Photon". In view of these results, we propose to study pion and photon dissociation at energies up to 300 GeV. The TPL beam line is equipped to deliver electrons of this energy. The electrons are produced by intercepting a secondary neutral beam with a thin radiator. In E-612, the pion beam was formed by replacing the radiator with four inches of lead. This beam was accompanied with an electro-magnetic halo, which limited the flux of pions that could be accepted by the apparatus to $\sim 5 \times 10^4$ per pulse. In order to decrease the background accompanying the pions, we propose to run with a pion beam which is produced directly from the primary protons. We understand that this can be done at little expense. An added advantage of this method is that the required primary beam intensity will be small.

The main purpose of the proposed study is to understand better our E-612 results on the finite mass sum rule (FMSR) and factorization. At twice the energy, the M_x^2 extent of the diffractive region doubles. Hence, the high mass $1/M_x^2$ behavior will be checked better and a more reliable extrapolation into the low mass region will be made. It will be interesting to test the FMSR at various values of t. The importance of this test in

relation to "the shape of the ρ" has been emphasized in our paper[1]. The test of factorization in our E-612 experiment does not give an accurate value of the "effective photon mass", M_0. We would like to perform this test well and compare the value of M_0 with that obtained from the FMSR.

The charged multiplicity distributions of pion and photon diffractive masses will be measured up to $M_x^2 = 0.1s = 56\ \mathrm{GeV}^2$. Direct comparison of the charged multiplicities provides a test of the universality hypothesis[2].

In the course of the above study, small t pion elastic scattering will also be measured. The world data on the slope parameter of $\pi^- p$ elastic scattering at $|t| \sim 0.05\ (\mathrm{GeV/c})^2$, shown[3] in Figure 1, are not good enough to allow a definite conclusion to be drawn about the equality of the increase of the slope parameter with energy for $\pi^- p$ and pp elastic scattering. We propose to measure b for $\pi^- p \to \pi^- p$ at energies from 50 to 300 GeV. Even in the presence of possible small systematic errors, such a measurement will give the correct energy dependence of the slope.

In determining the desired length of the proposed run, the quality of the beam is a key factor. We feel that, with a good pion beam and a photon beam similar to the one we had in E-612, an amount of time comparable to that spent in E-612 would be required; i.e., about two to three months. Thus, the second half of the 1983-1984 running period indicated "OPEN" for TPL in the 11/13/82 tentative schedule, should be sufficient. If the high energy tagged photon beam intensity is not high enough during this period. we intend to ask for more time in the second half of the 1984-1985 running period to complete the photon part of the experiment.

REFERENCES

1. T. Chapin et al., "Diffraction Dissociation and The Direct Hadronic Interaction of the Photon".
2. K. Goulianos, "Diffractive Interactions of Hadrons at High Energies." (Contributed paper at The International Conference on High Energy Physics, Paris, France, July 26-31, 1982 - Rockefeller University Report No. RU 81/A-23.
3. K. Goulianos et al., "Universality of Charged Multiplicity Distributions," Phys. Rev. Letters 48, 1454 (1982).

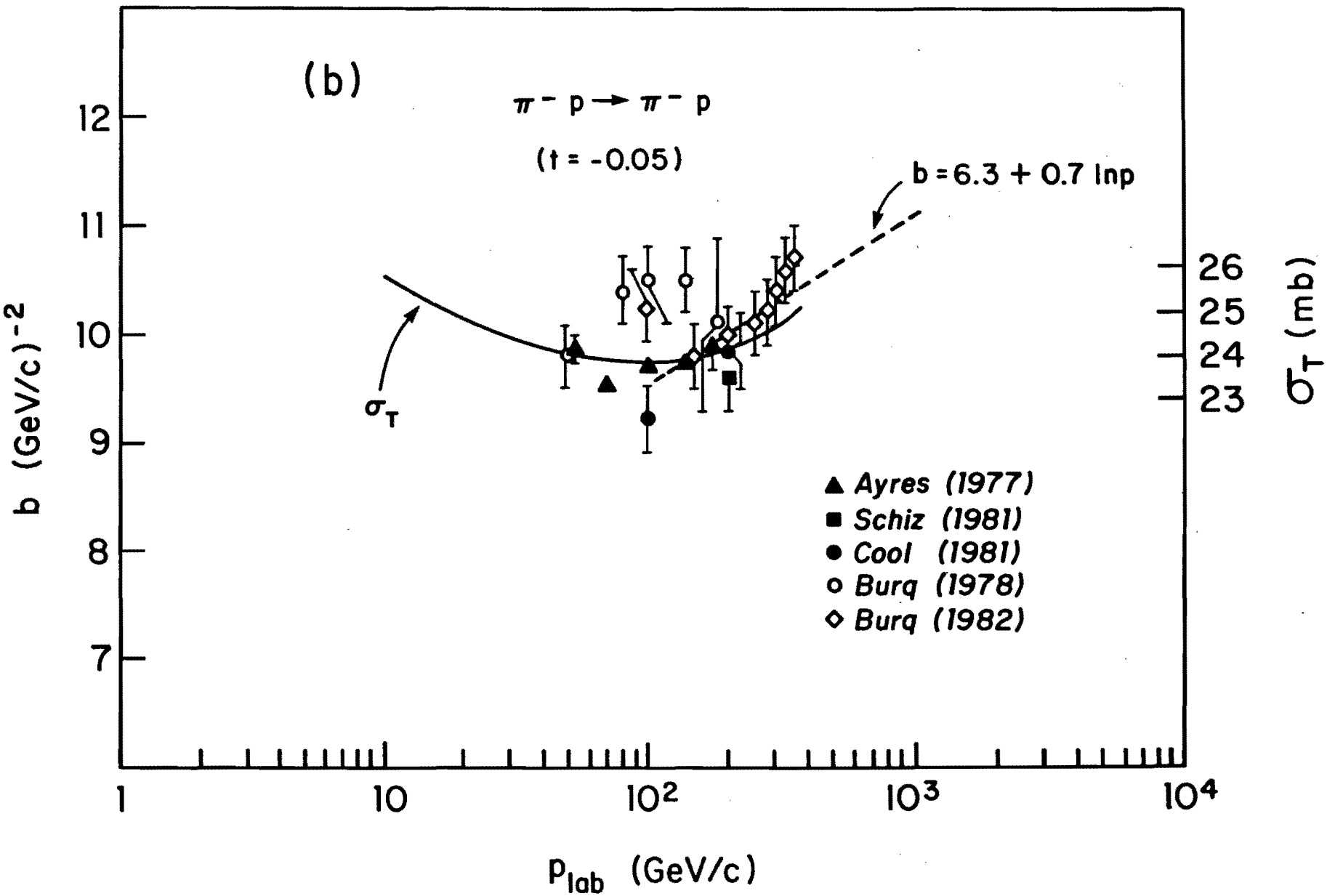

FIG. 1 - Slope parameter of $\pi^- p \rightarrow \pi^- p$ at $|t| \sim 0.05$ (GeV/c)^2 as a function of laboratory momentum (from Reference 2).

DIFFRACTION DISSOCIATION
and
THE DIRECT HADRONIC INTERACTION OF THE PHOTON

K. Goulianos*

The Rockefeller University
New York, N.Y. 10021, U.S.A.

Invited paper presented at
The XVIIIth Rencontre de Moriond on Gluons and Hadron Physics
Session 1, January 23-29, 1983
La Plagne, Savoie, France

ABSTRACT

We report a measurement of the inclusive diffraction dissociation cross section of $\sim$ 100 GeV photons on hydrogen; we test the finite mass sum rule and, comparing with pion dissociation data, we test factorization. Our results are interpreted as providing a measurement of the direct, non "vector-meson dominance" hadronic interaction of the photon.

*Report on Fermilab Experiment E-612:

T. Chapin, R. Cool, K. Goulianos, K. Jenkins,
J. Silverman, G. Snow, H. Sticker and S. White

The Rockefeller University
New York, N.Y. 10021, U.S.A.

and

Yue Hua Chou
Institute of High Energy Physics, Beijing
The People's Republic of China

In an experiment performed at Fermilab, E-612, we measured the inclusive diffraction dissociation cross section $d^2\sigma/dtdM_x^2$ of $\sim$100 GeV photons incident on protons,

$$\gamma + p \rightarrow X + p \tag{1}$$

in the kinematic range $0.02 < |t| < 0.1$ $(GeV/c)^2$ and $M_x^2/s \lesssim 0.1$. As a control experiment, we also measured, in the same apparatus, the pion diffraction dissociation cross section,

$$\pi^- + p \rightarrow X + p \tag{2}$$

at 100 GeV/c. Pion dissociation has been measured previously[1]; this experiment represents the first measurement of inclusive photon dissociation at high energies.

We find that, for $M_x^2 > 4$ GeV^2, the differential cross sections for both reactions vary as $1/M_x^2$ and are exponential in t, a behavior consistent with that predicted by a simple triple-Pomeron Regge type amplitude. By applying the finite mass sum rule to the photon data, and by comparing the photon with the pion data to test factorization, we conclude that the photon has a direct hadronic interaction in addition to that described by the well known[2] vector-meson dominance model (VDM).

The experiment was performed in the tagged photon beam of Fermilab. The photons were obtained from an 148 GeV/c electron beam incident on a 20% tungsten radiator. The energy of the photons was determined to ±2% by bending the radiating electrons out of the beam and measuring their energy with lead glass counters. Typically, the photon beam contained

$\sim 1 \times 10^6$ tagged photons per pulse in the energy range $75 < E_\gamma < 148$ GeV. With the Bremsstrahlung energy spectrum varying as 1/E, the mean energy of the photons was ~ 100 GeV. The photon flux was limited by the rate capability of our detector. Double photon production in the radiator was monitored by a total absorption counter which, placed in the photon beam downstream of our apparatus, measured the total energy of the non-interacting photons. The pion beam was formed by intercepting the secondary neutral beam, which created the electrons, with a 5 cm lead brick. An electromagnetic halo accompanying the beam limited the acceptable flux of pions to $\sim 5 \times 10^4$ per pulse. The pulse repetition period of the machine was ~ 10 sec and the beam spill time ~ 1 sec. Data were collected in two runs of approximately equal duration, one during the month of January and the other during March of 1982.

The experimental technique consisted in measuring the kinetic energy and polar angle of recoil protons in the region $10 < T < 50$ MeV and $45^0 < \theta < 90^0$. The variables t and M_x^2 were then determined from T, θ and p_o, the momentum of the beam particle, using the equations

$$t = -2M_p T \tag{3}$$

$$M_x^2 = M_o^2 + 2p_o \sqrt{|t|} \left(\cos\theta - \sqrt{|t|}/2M_p\right) \tag{4}$$

where M_p is the mass of the recoil proton and M_o the mass of the incident particle.

The apparatus, TREAD (The Recoil Energy and Angle Detector), shown in Figure 1, was described in detail in a previous publication[3]. It is a hydrogen filled, high pressure time projection chamber (TPC) that served

both as target and as detector of the recoil protons. It consists of two cylindrical drift regions in tandem, each 45 cm in diameter and 75 cm long. The beam entered the TPC alaong the axis of the cylinder through a 0.75 mm thick, 5 cm dia. beryllium window and exited through a 2 mm thick, 20 cm dia. aluminum window. The dissociation products also exited through the aluminum window, whereupon their charged multiplicity was determined by measuring the pulse height in two scintillation counters. This technique was used previously[4] by some members of this group in a hadron experiment, E-396, performed at Fermilab's meson laboratory. The energy of the recoil protons was determined by stopping them in 2.5 cm thick plastic scintillation counters located inside the pressure vessel. The energy loss in the hydrogen gas, dE/dx, was obtained from the pulse height of the sense wires. Recoiling protons were identified by comparing T with dE/dx.

In this report we present the result of the analysis of the data collected during March 1982. The data obtained in January of 1982 are currently being analyzed. Details of the analysis will be given elsewhere[5]. Basically, after track selection and appropriate cuts in dE/dx versus E and in recoil time of flight, the background was negligible.

Figure 2 is a scatter plot of the recoil kinetic energy against dE/dx for the photon data. The prominent band represents the recoil protons for which the energy loss varies as 1/T. Multiplying dE/dx by T yields a constant which is proportional to the mass of the recoil particle. Figure 3 is a histogram of (dE/dx) · T. The peak consists of recoil protons. Its width is mainly due to the dE/dx measurement resolution.

The M_x^2 distributions of the pion and photon data, normalized respectively to the $\pi^- p$ and γp total cross sections, are shown in Figure 4. The data, representing about 7,500 pion and 8,500 photon events, are plotted against the cross-symmetric variable ν ,

$$\nu = M_x^2 - M_o^2 - t \tag{5}$$

where M_o is the mass of the incident particle. The width of the pion elastic peak at $\nu \cong 0$ and of the ρ-meson peak at $\nu \cong 0.6$ GeV^2 are mostly due to the measurement resolution. The resolution is poorer in the photon data, which were collected over a period of one month, than in the pion data, collected during one day. In the Regge model, under the assumption of factorization, the high mass diffraction dissociation cross-section arising from a triple-Pomeron term can be written as

$$\frac{d^2\sigma^{hp}}{dtd\nu} = \frac{\beta_{hP}(o) \quad \beta^2{}_{pP}(t) \quad G_{PPP}(t)}{16\pi\nu} \tag{6}$$

where h represents the hadron dissociating on the proton and P represents the Pomeron. In the same model, the total cross section at high energies is given by

$$\sigma_T^{hp} = \beta_{hP}\ (o) \quad \beta_{pP}\ (o) \tag{7}$$

In writing (6) and (7), we have taken, for simplicity, the Pomeron trajectory to be $\alpha(o) = 1$ and, because of our small t values, the slope of the trajectory to be $\alpha'(t) = 0$. The ratio of the diffractive to the total cross section,

$$\frac{d^2\sigma^{hp}/dt\ d\nu}{\sigma_T^{hp}} = \frac{\beta_{pP}^2(t)}{\beta_{pP}(o)} \quad \frac{G_{PPP}(t)}{16\pi\nu} \tag{8}$$

is independent of the incident particle type. The $1/\nu$ behavior predicted by Eq. (6) and the scaling of the diffractive to the total cross section given by Eq. (8) have been found to hold for $\pi^{\pm}$, $K^{\pm}$, and $p^{\pm}$ hadrons dissociating on protons[1]. Figure 4 shows that the high mass diffractive photon cross section is $\sim$15% higher than the pion cross section (scaled by the corresponding σ_T). This could, of course, be considered as a positive test of factorization in view of the fact that the photon total cross section is $\sim$200 times smaller than the pion cross section. However, this discrepancy finds a logical explanation in the framework of the vector-meson dominance model.

In its original version, the VDM states that the hadronic interaction of the photon is transmitted through the coupling of the photon to the vector mesons ρ, ω and ϕ. For simplicity, we will consider only the ρ-meson in this discussion. A photon cannot transform into a ρ in free space. Conversion to ρ requires an energy change $\Delta E = M_\rho^2/2E_\gamma$. For 100 GeV photons, ΔE = 3 MeV. Through the uncertainty principle, $\Delta E \cdot \Delta t \sim 1$, this energy shift corresponds to a time interval which is large compared to the characteristic time of strong interactions set by the mass of the pion (140 MeV). Thus, high energy photons can live in and interact with nuclear matter as "free" ρ-mesons. Of course, photons can also interact directly. Therefore, the effective "incident photon" mass, M_0^2, lies somewhere between zero and M_ρ^2. Assuming that there is no interference between the γ and ρ amplitudes, the value of M_0^2 is given by

$$M_0^2 = \frac{P_\gamma \sigma_\gamma^D M_\gamma^2 + P_\rho \sigma_\rho M_\rho^2}{P_\gamma \sigma_\gamma^D + P_\rho \sigma_\rho} = \frac{P_\rho \sigma_\rho M_\rho^2}{\sigma_\gamma^T} \tag{9}$$

where $P_{\gamma,\rho}$ are the probabilities of finding the photon in the $\gamma(M_\gamma^2 = 0)$ or $\rho(M_\rho^2 = 0.59\ \mathrm{GeV}^2)$ states and σ_γ^D is the "direct" γ total cross section. The VDM assumes that $P_\rho \sigma_\rho >> P_\gamma \sigma_\gamma$ and hence $M_0^2 \cong M_\rho^2$. Had we used M_ρ^2 instead of M_γ^2 in Figure 4, the photon data would be in agreement with the pion data. Thus, assuming the validity of factorization and of the Regge model, this result supports the VDM. However, it is not sensitive enough to rule out a direct photon interaction of $\sim$20% which is required to explain the shadowing of photons in nuclei[2]. Such an interaction is also desirable in the simple VDM which can account for only $\sim$80% of the photon total cross section, although this inadequacy can be corrected by introducing the generalized VDM[2]. A more sensitive measurement of M_0^2, and hence of the direct photon interaction, is provided by our data through the application of the finite mass sum rule (FMSR).

The FMSR[6] relates the high mass diffractive cross section to the low mass "resonance region." It states that the fit to the large ν differential cross section, $d^2\sigma/dtd\nu$, multiplied by ν represents the average behavior of $\nu(d^2\sigma/dtd\nu)$ in the low mass region, including elastic scattering for which $\nu = |t|$:

$$|t| \frac{d\sigma_{e\ell}}{dt} + \int_0^{\nu'} \nu \frac{d^2\sigma}{dtd\nu}\, d\nu = \int_0^{\nu'} \nu \left(\frac{d^2\sigma}{dtd\nu}\right)_{\text{fit at large } \nu} d\nu \tag{10}$$

The value of ν' must lie beyond the "resonance region" but is otherwise arbitrary. However, the lower the value of ν' the more sensitive the test of the FMSR. The elastic contribution appears explicitly in Eq. (10). Experimentally, due to resolution in the measurement of M_x^2, elastic scattering appear as a peak of finite width in ν centered around $\nu = |t|$. In applying the FMSR, the elastic events can be treated just as the inelastic ones; namely, by multiplying the apparent cross section $d^2\sigma/dtd\nu$ by $\nu = M_x^2 - M_o^2 + |t|$ and integrating over ν down to values which are low enough to include all events. For a resolution broadened peak which is symmetric around $M_x = M_o$, the elastic events in this procedure are, in effect, multiplied by $|t|$, as required by the FMSR. Thus, in applying the FMSR to experimental data, Eq. (10) can be written as

$$R \equiv \frac{\int^{\nu'} \nu \frac{d^2\sigma}{dtd\nu} d\nu}{\int_o^{\nu'} \nu \left(\frac{d^2\sigma}{dtd\nu}\right)_{\text{fit at large } \nu} d\nu} = 1 \qquad (11)$$

where the lower limit of integration in the numerator has been omitted but it is understood that one must sum over all events below ν', including the elastic events that are forced by the resolution to appear at negative values of ν.

Figures 5a and 5b show $\nu(d^2\sigma/dtd\nu)$ for our pion and photon data plotted against $\nu = M_x^2 - M_{\pi,\gamma}^2 + |t|$. For $\nu \gtrsim 4$ GeV, our data for both reactions are flat, implying an $1/\nu$ behavior of $d^2\sigma/dtd\nu$ and hence

triple-Pomeron dominance in the diffractive cross sections. The $A_1(M^2=1.63)$ and ρ' $(M^2=2.56)$ peaks are clearly visible in the pion and photon data, respectively. Applying the FMSR with $\nu' = 4\ \mathrm{GeV}^2$, we find $R_\pi = 1.10 \pm 0.05$ and $R_\gamma = 1.43 \pm 0.04$. Clearly, in this straightforward application, the FMSR fails for the photon data. We attribute this failure to the fact that, as discussed previously, the photon interacts partly as a ρ-meson and therefore $\nu = M_X^2 - M_0^2 - t$, where M_0^2 is given by Eq. (9). Treating M_0^2 as a free parameter and demanding the validity of the FMSR, i.e., $R = 1$ in Eq. (10), we find $M_0^2 = 0.46 \pm 0.02\ \mathrm{GeV}^2$. From Eq. (9), we then find $P_\rho\sigma_\rho/\sigma_\gamma^T = M_0^2/M_\rho^2 = (0.46 \pm 0.02)/0.59 = 0.78 \pm 0.035$ and consequently

$$\sigma_\gamma^D = (0.22 \pm 0.035)\ \sigma_\gamma^T \tag{12}$$

i.e., the direct hadronic photon cross section is $22 \pm 3.5\%$ of the total. As mentioned earlier, this value is in agreement with results on shadowing of photon total cross sections in nuclei and with the fact that the simple VDM accounts for only $\sim 80\%$ of the total photon cross section.

The t distributions were fitted to the simple exponential form e^{bt}. Figure 6 shows the slope parameter b as a function of M_X^2. The pion elastic scattering and high mass diffraction slopes are in good agreement with the values of 8.92 ± 0.31 and $4.3 \pm 0.7\ (\mathrm{GeV}/c)^{-2}$ measured[7] in experiment E-396. The slope at $M_X^2 \cong 0.8\ \mathrm{GeV}^2$ was obtained from pion data with charged multiplicity ≥ 3 in order to exclude events from the nearby elastic peak. The large value of the slope in this low mass inelastic region is essential in satisfying the FMSR at small values of t. From Eq. (10), it is

seen that as $|t| \to 0$ the elastic contribution vanishes; however, due to the large value of the slope of the low mass inelastic region, the relative contribution of this region increases at small t and the FMSR is satisfied. Our present data are not accurate enough to provide a stringent test of the FMSR as a function of t. Such a test was performed[8] for $pp \to Xp$; it was found that the slope parameter of the low mass region was indeed high and its magnitude was exactly what was required to satisfy the FMSR.

In examining the slope parameters of the photon dissociation data, we observe the following:

(i) The slopes of the high mass photon and pion data are in agreement.

(ii) The slope at the mass of the ρ-meson (M_X^2=0.59) is about one unit higher than the pion elastic scattering slope, although the statistical significance of this difference is not very high.

(iii) There is no increase of the slope in the region $M_X^2 > M_\rho^2$.

The M_X^2 dependence of b does not follow exactly the pattern set by the hadron data. The slope is not higher in the region just above the ρ mass and, in this sense, the ρ' does not correspond to the A_1 enhancement.

Following the argument presented previously, it would then appear that the FMSR would be violated at small values of t. However, data from experiments at lower energies (see Fig. 7) indicate that the slope in the mass region $M_X^2 < M_\rho^2$ is higher than the slope of the ρ. Our experimental resolution does not permit us to observe directly this increase of slope at low masses, but indirect evidence is provided by the fact that the measured

slope of the ρ is larger than that of pion elastic scattering. Thus, the low mass "tail" of the ρ in $\gamma p \to Xp$ may indeed play the role of the A_1 and N^* (1400) enhancements observed in $\pi p \to Xp$ and $pp \to Xp$, respectively.

As menionted earlier, we also measured in this experiment the pulse height in two scintillation counters placed downstream of TREAD in order to determine the charged multiplicity of the dissociation products. Figure 8 shows the pulse height spectra for the photon and pion data in the region $3 < M_X^2 < 10\ \mathrm{GeV}^2$ in units corresponding to minimum ionizing particles. In order to extract the multiplicity distribution, these spectra must be fitted with appropriate Landau functions. However, a direct comparison of the photon and pion data, which in Figure 8 are normalized to the same number of events, already shows that the charged multiplicity distribution has the same mean value and the same width for both reactions. This result is in agreement with the "Universality of Charged Multiplicity Distributions" shown to hold for hadronic masses[9].

In summary, we find that $d^2\sigma/dtd\nu$ for $\gamma(\pi^-) + p \to X + p$ at 100 GeV/c varies as $(1/\nu)\ e^{bt}$, in agreement with a triple-Pomeron amplitude; by testing factorization and the FMSR, we conclude that the effective mass of the incident photon is $M_0^2 = 0.46 \pm 0.02\ \mathrm{GeV}^2$ and, by comparing with M_ρ^2, we determine the direct, non-VDM hadronic cross section of the photon to be 22 ± 3.5% of the total cross section; from a study of the t-distributions, combined with results from experiments at lower energies, we argue that the low mass "tail" of the ρ-meson is the counterpart of the low mass enhancements A_1 and N^* (1400) observed in $\pi^-(p) + p \to X + p$; finally, from the pulse height spectra in the "multiplicity counters", we verify the universality character of the charged multiplicity distributions for the case of photons.

REFERENCES

1. R.L. Cool, K. Goulianos, S.L. Segler, H. Sticker and S.N. White, Phys. Rev. Letters 47, 701 (1981).
2. T.H. Bauer, D. Spital, D.R. Yennine and F.M. Pipkin, Reviews of Modern Physics 50, 26, (1978).
3. T. Chapin et al., Nuclear Instruments and Methods 197, 305 (1982).
4. R.L. Cool, K. Goulianos, S.L. Segler, H. Sticker and S.N. White, Phys. Rev. Letters 48, 1451 (1982).
5. Gregory Snow, Ph.D. Thesis, Rockefeller University (in preparation).
6. A.I. Sanda, Phys. Rev. D6, 280 (1972); M.B. Einhorn, J. Ellis and J. Finkelstein, ibid. 5, 2063 (1972).
7. R.L. Cool, K. Goulianos, S.L. Segler, G. Snow, H. Sticker and S.N. White Phys. Rev. D24, 2821 (1981).
8. Y. Akinov et al., Phys. Rev. D14, 3148 (1976)
9. K. Goulianos, H. Sticker and S.N. White, Phys. Rev. Letters 48, 1454 (1982).

FIGURE CAPTIONS

FIG. 1 - TREAD (The Recoil Energy and Angle Detector).

FIG. 2 - Recoil particle energy loss, dE/dx, versus kinetic energy. The prominent band represents recoil protons.

FIG. 3 - Recoil particle energy loss times kinetic energy, $(dE/dx)\cdot T$. This product is proportional to the mass of the recoil particle. The position of the peak is normalized to unity so that the abseissa represents M(recoil)/M(proton).

FIG. 4 - M_X^2 distributions for $\gamma(\pi^-) + p \to X + p$ at 100 GeV/c and $0.02 < |t| < 0.1$ $(GeV/c)^2$, normalized to the corresponding total cross sections, $\gamma(\pi^-) + p \to$ anything.

FIG. 5 - Test of the finite mass sum rule: The product $\nu(d^2\sigma/dtd\nu)$, where $\nu = M_X^2 - M_{\pi,\gamma}^2 + |t|$, plotted against ν (a) for $\pi^- p \to Xp$ and (b) for $\gamma p \to Xp$ at 100 GeV/c and $0.02 < |t| < 0.1$ $(GeV/c)^2$.

FIG. 6 - The slope parameter b as a function of M_X^2 for $\gamma(\pi^-) + p \to X + p$ at 100 GeV/c and $0.02 < |t| < 0.1$ $(GeV/c)^2$.

FIG. 7 - The "shape of the ρ" as a function of t (from Reference 2).

FIG. 8 - Pulse height spectra ("charged multiplicities") of the dissociation products for $\gamma(\pi^-) + p \to X + p$ at 100 GeV/c in the region $3 < M_X^2 < 10$ GeV^2.

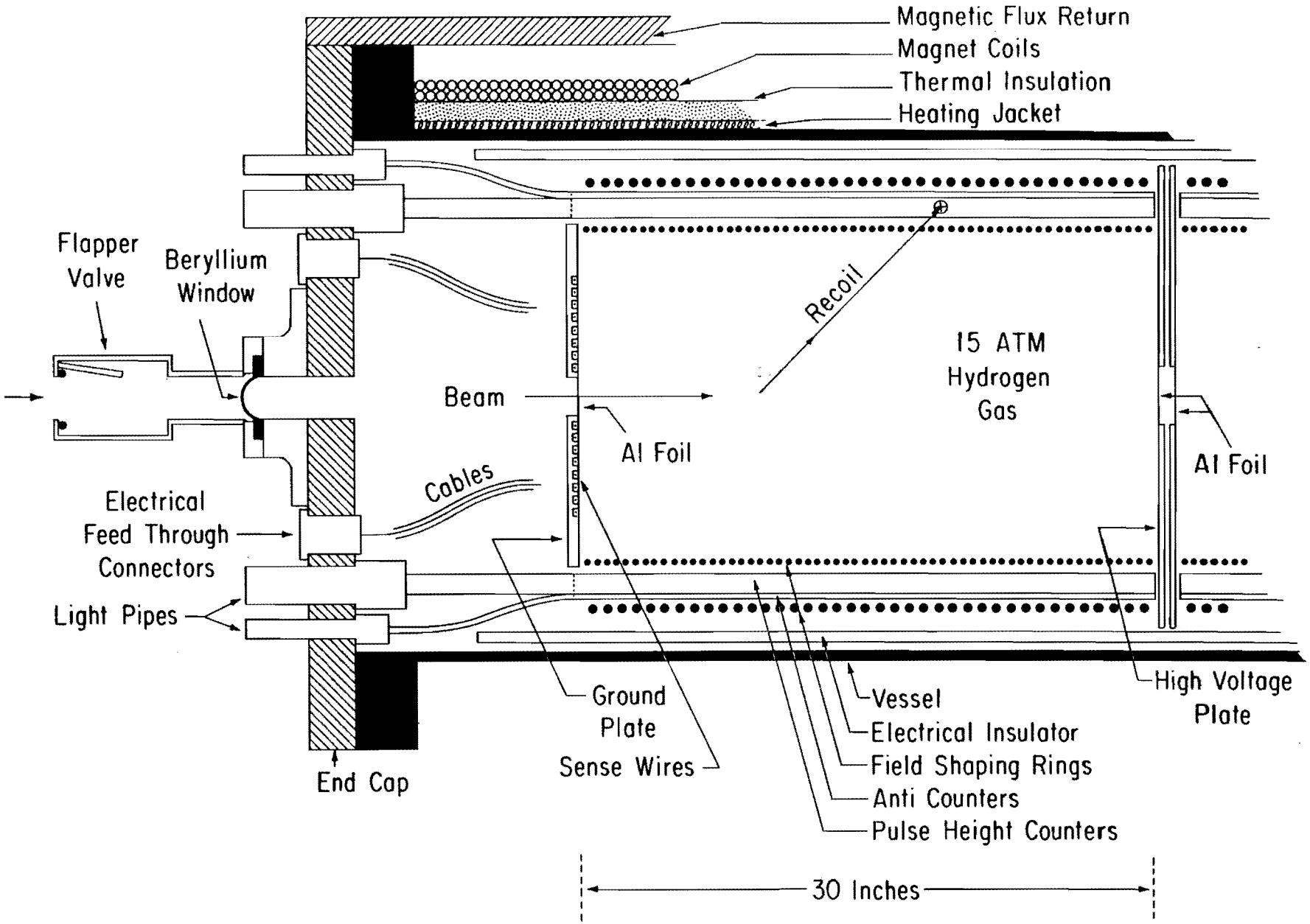
Magnetic Flux Return
Magnet Coils
Thermal Insulation
Heating Jacket
Flapper Valve
Beryllium Window
Recoil
15 ATM Hydrogen Gas
Beam
Al Foil
Al Foil
Cables
Electrical Feed Through Connectors
Light Pipes
Ground Plate
Sense Wires
Vessel
Electrical Insulator
Field Shaping Rings
Anti Counters
Pulse Height Counters
High Voltage Plate
End Cap
30 Inches

FIG. 1

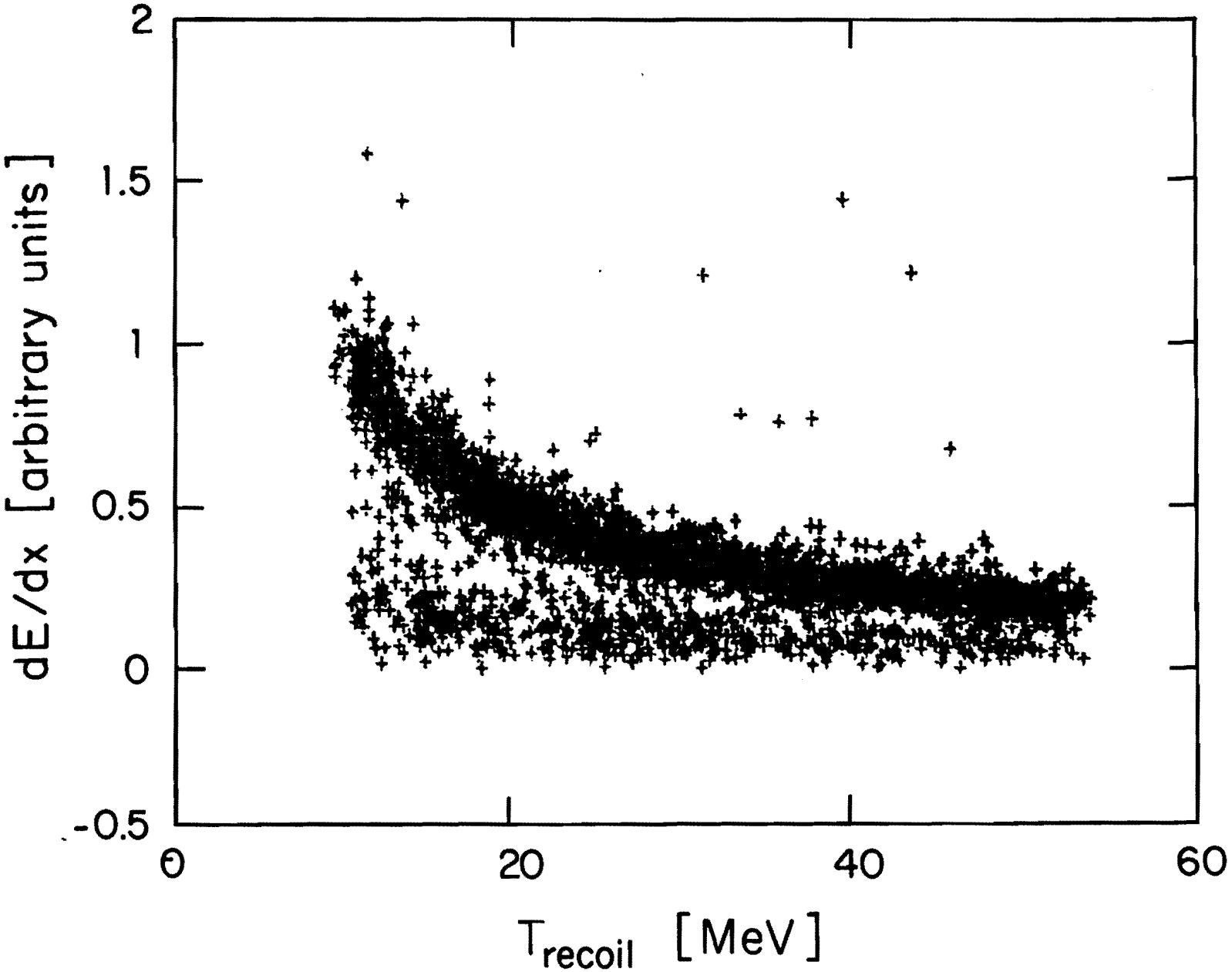

FIG. 2

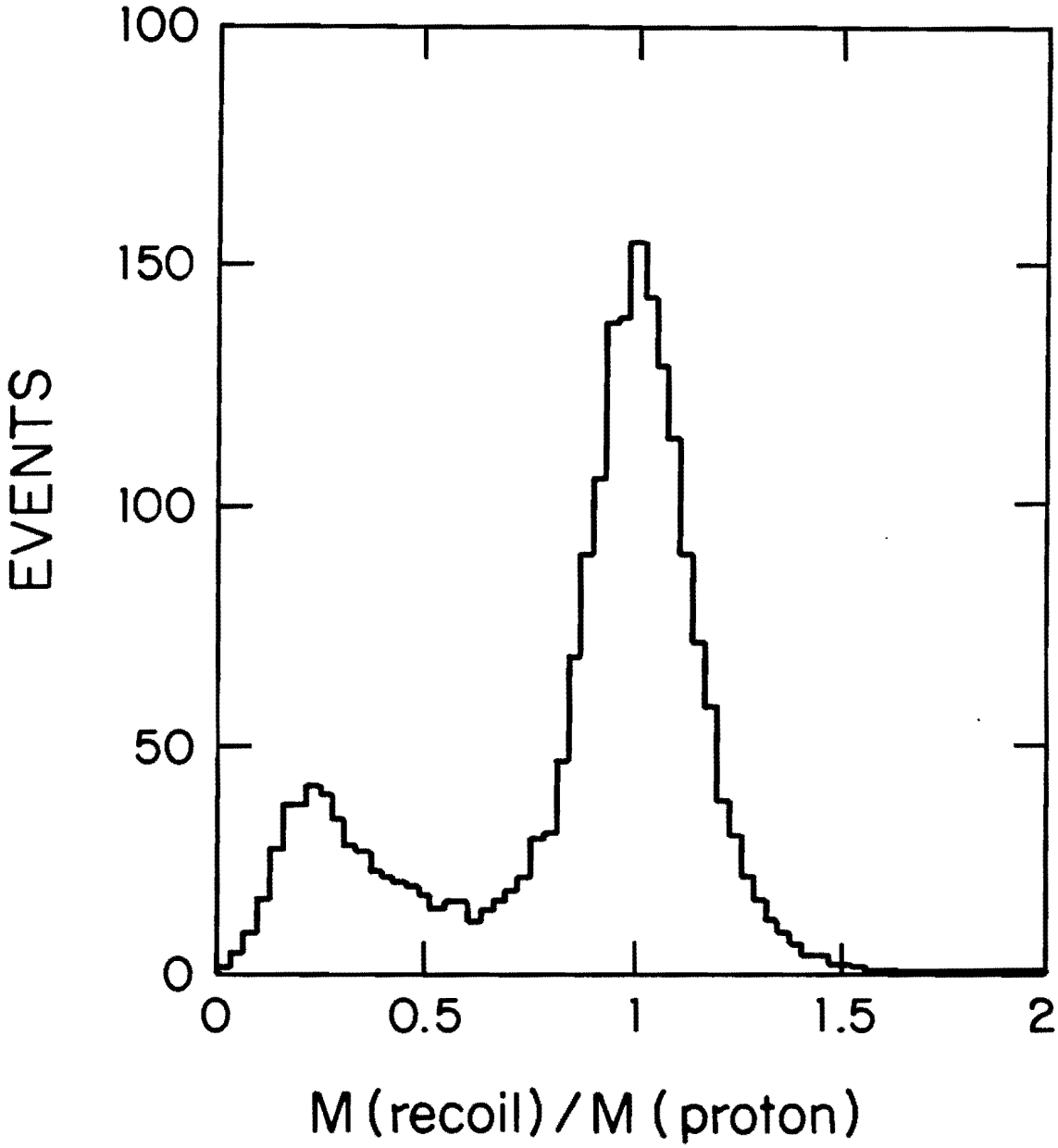

FIG. 3

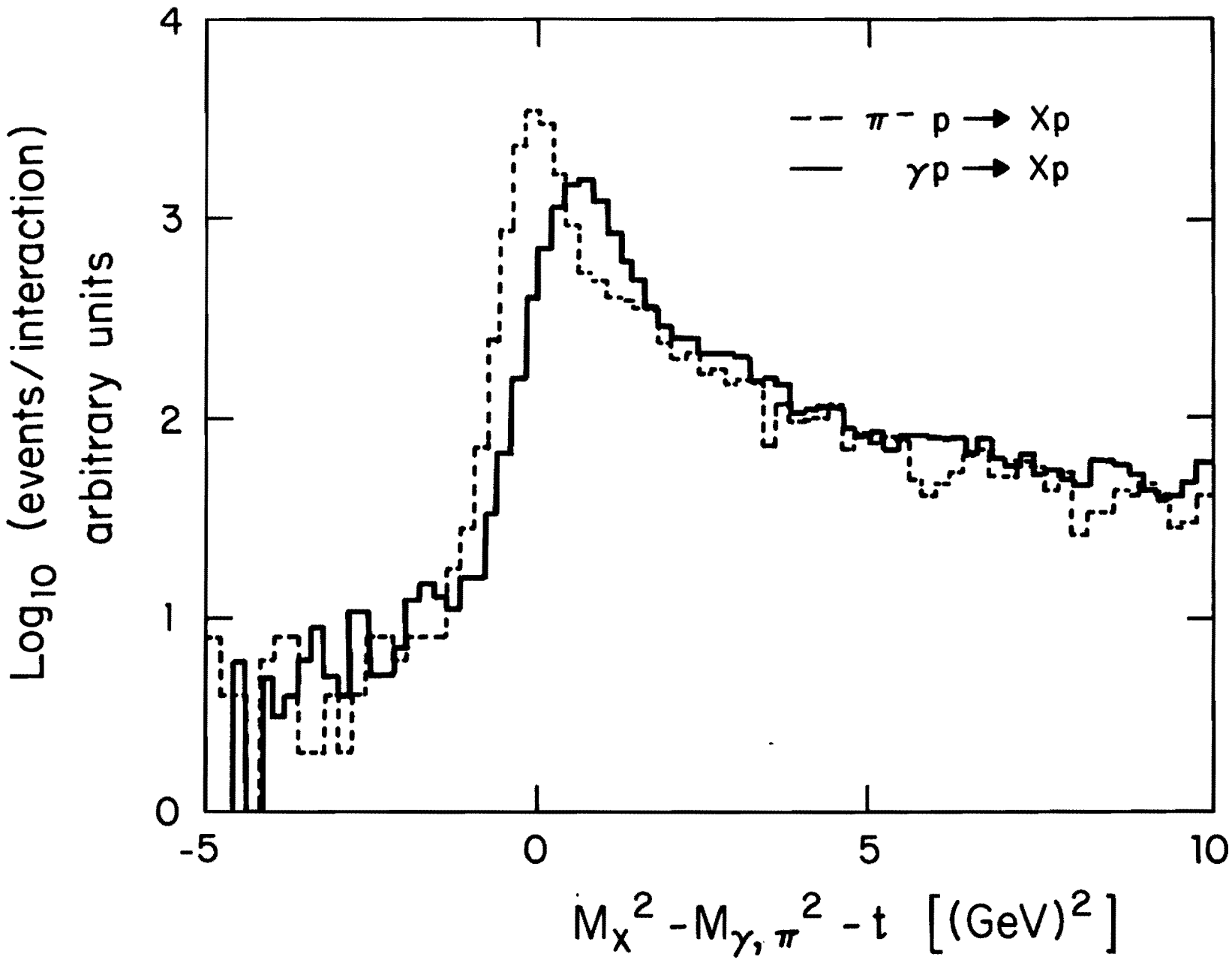
4
3
2
1
0
-5
0
5
10
Log10 (events/interaction)
arbitrary units
π⁻ p → Xp
γp → Xp
Mx² - Mγ,π² - t [(GeV)²]

FIG. 4

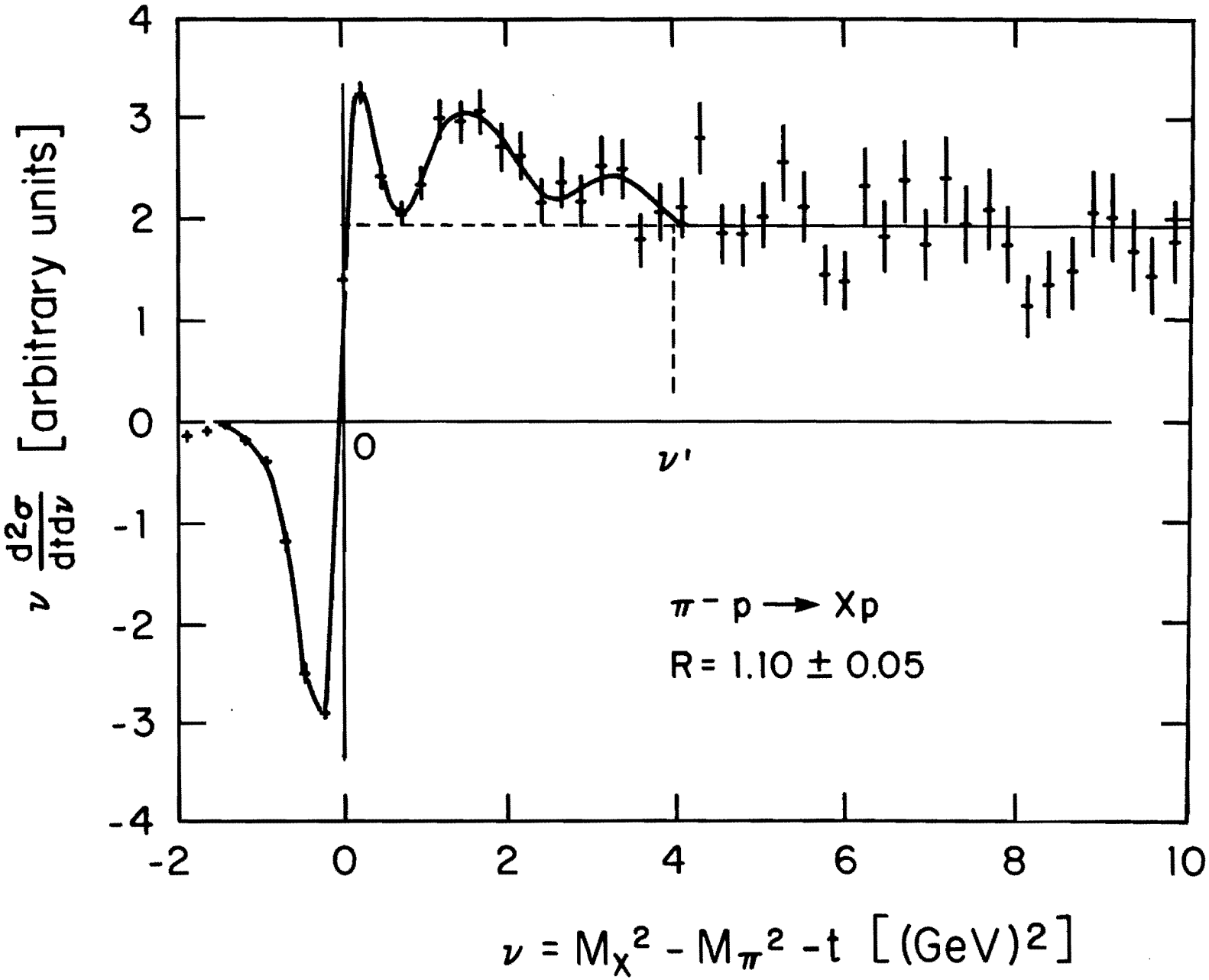
4
3
2
1
0
-1
-2
-3
-4
-2
0
2
4
6
8
10
0
ν'
π⁻ p → Xp
R = 1.10 ± 0.05
ν d²σ/dtdν [arbitrary units]
ν = M_X² - M_π² -t [(GeV)²]

FIG. 5a

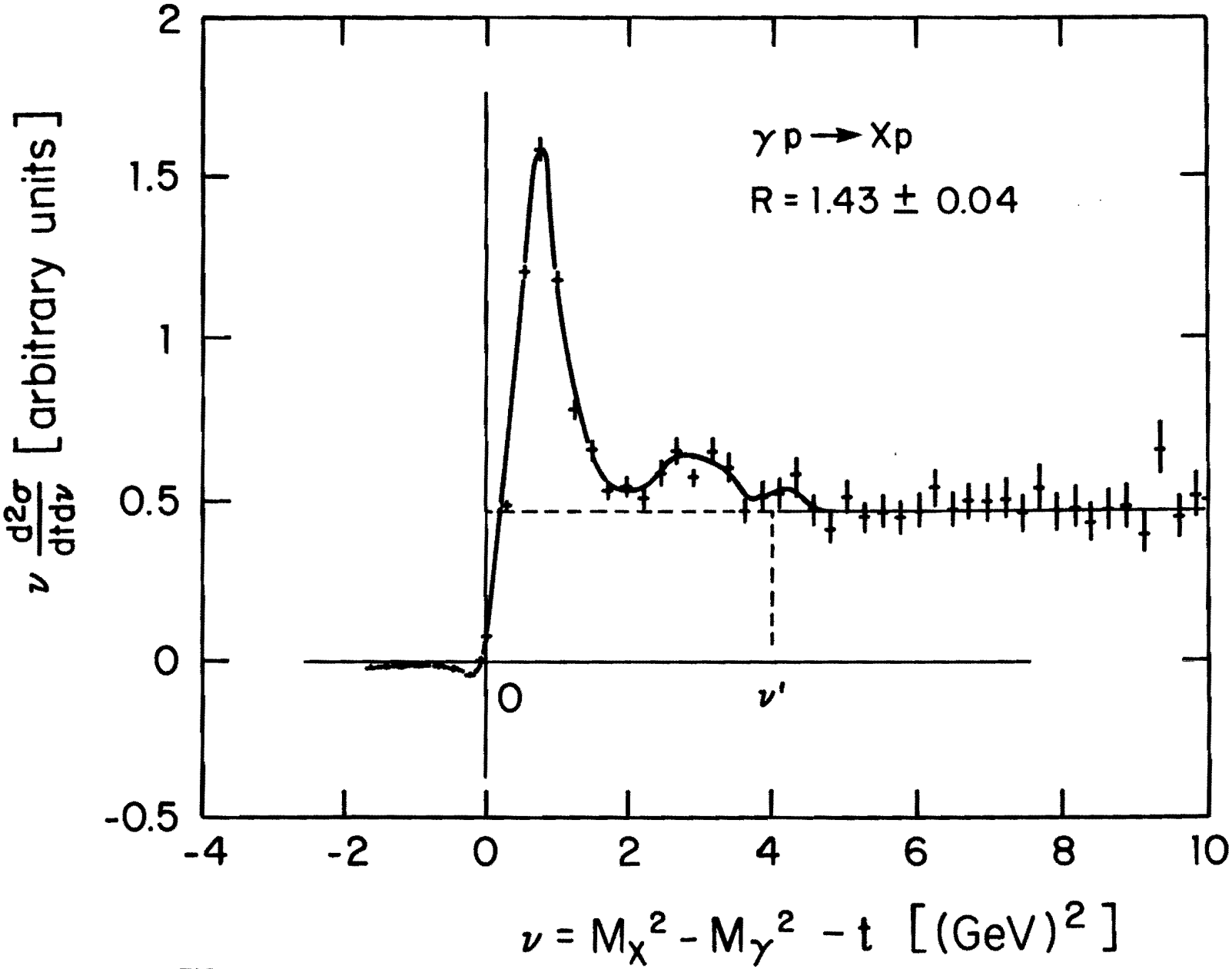
γp → Xp
R = 1.43 ± 0.04
ν d²σ/dtdν [arbitrary units]
ν = M_X² - M_γ² - t [(GeV)²]
0
ν'
2
1.5
1
0.5
0
-0.5
-4
-2
0
2
4
6
8
10

FIG. 5b

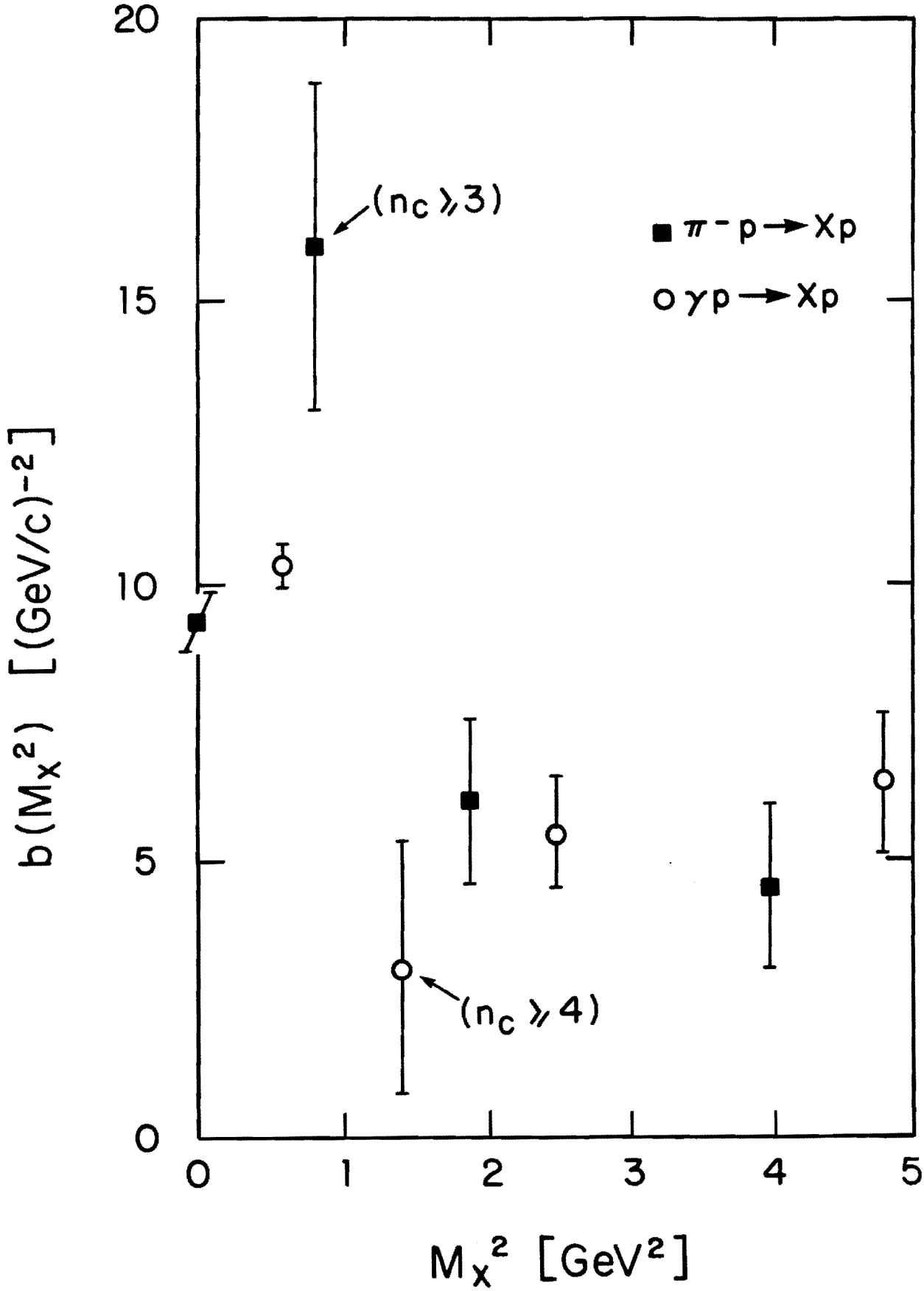
20
15
10
5
0
0
1
2
3
4
5
$b(M_X^2)$ [(GeV/c)$^{-2}$]
M_X^2 [GeV^2]
($n_c \geq 3$)
($n_c \geq 4$)
■ $\pi^- p \rightarrow Xp$
○ $\gamma p \rightarrow Xp$

FIG. 6

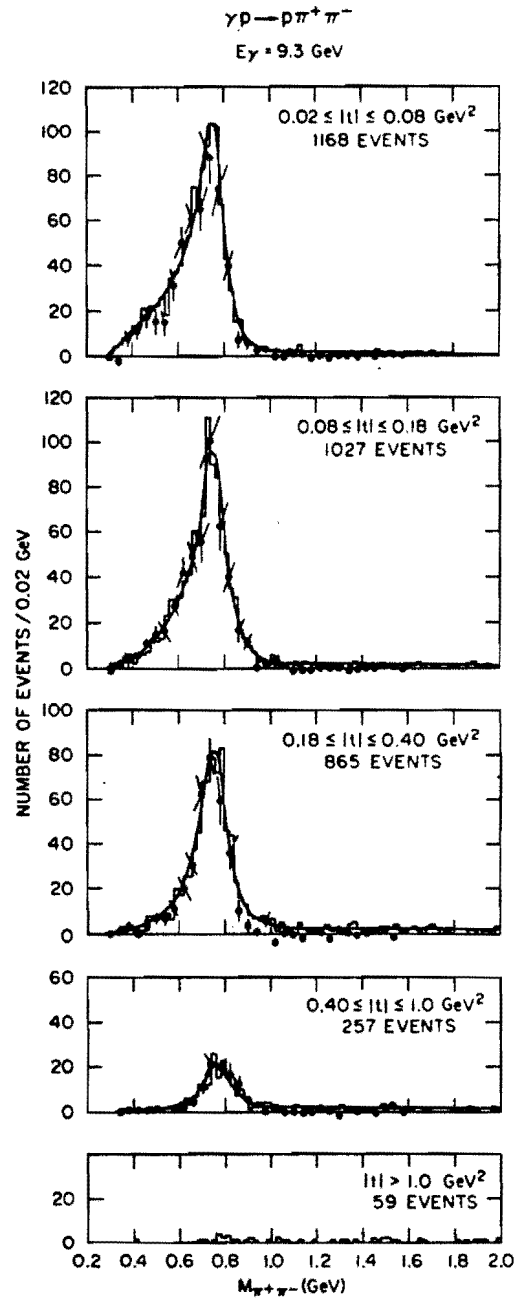

FIG. 70. Reaction $\gamma p \to p\pi^+\pi^-$ at 9.3 GeV. Distributions of the $\pi^+\pi^-$ mass for different t intervals. The helicity-conserving p-wave intensity, Π, is shown by the solid points. The curves give the result of a maximum-likelihood fit to the reaction using the Söding model (from Ballam *et al.*, 1973).

FIG. 7

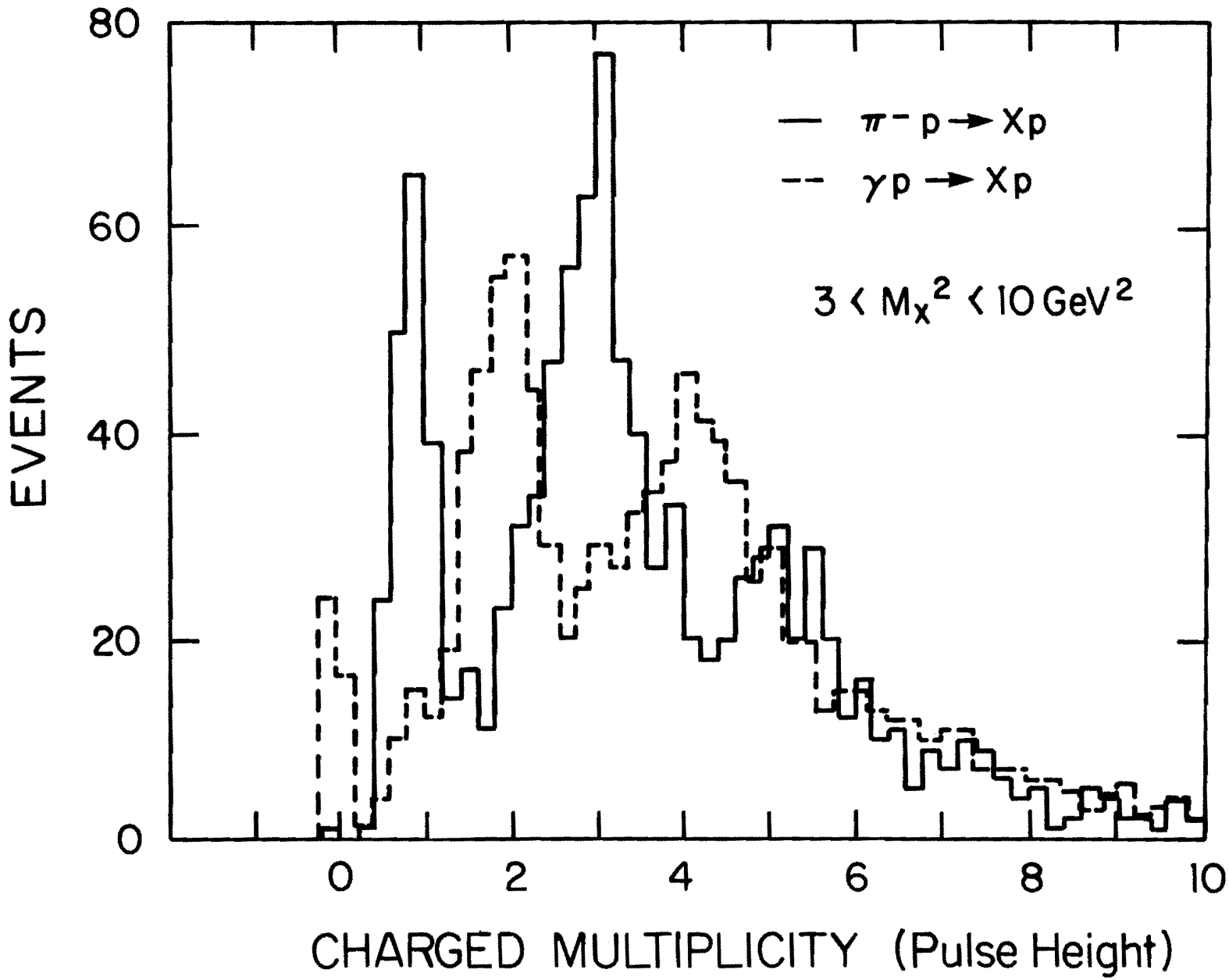
80
60
40
20
0
EVENTS
0
2
4
6
8
10
CHARGED MULTIPLICITY (Pulse Height)
— $\pi^- p \rightarrow Xp$
-- $\gamma p \rightarrow Xp$
$3 < M_X^2 < 10\,GeV^2$

FIG. 8